Applied Ocean Research 99 (2020) 102125

Contents lists available at ScienceDirect

Applied Ocean Research

journal homepage: www.elsevier.com/locate/apor

A Bayesian wave inference method accounting for nonlinearity related inaccuracies in motion RAOs

J. Mas-Soler[a,b,*], Alexandre N. Simos[a]

[a] Naval Arch. & Ocean Eng. Department, Escola Politécnica da Universidade de São Paulo (USP), Brazil
[b] CEHINAV, ETSIN, Universidad Politécnica de Madrid (UPM), Spain

ARTICLE INFO

Keywords:
Directional wave spectra estimation
Bayesian inference
Non-linearity related inaccuracies of motion RAOs
Semisubmersible platform

ABSTRACT

Motion based wave inference allows the estimation of the directional sea spectrum from the measured motions of a vessel. Solving the resulting inverse problem is challenging as it is often ill-posed; moreover, inaccuracies related to the linearity hypothesis behind estimated platform response functions (RAOs) may result in misleading estimations of the sea states. This work discusses how these inaccuracies affect the estimations obtained by means of a Bayesian motion based wave inference method (VMB). For this purpose, an heuristic correction, accounting for the non-linearity related inaccuracies of the estimated RAOs, is included in an expanded Bayesian inference approach. Then, the resulting inference model is verified by means of a comparison between the outputs of this novel approach and those obtained without accounting for nonlinearity related inaccuracies in the RAOs. This assessment has been carried out using the data measured through dedicated model scale experiments of the Equinor's Åsgard-B semisubmersible oil processing platform. The results attested that improvements are obtained if the linearly related RAOs inaccuracies are taken into account in the VMB, especially for the sea conditions that excite the non-linear responses of the semisubmersible platform adopted as motion-based wave sensor.

1. Introduction

The knowledge of the sea conditions is of central importance for a wide range of offshore and nearshore operations, engineering design and validation of forecasts of extreme wave events. As a matter of fact, observed metocean data and analyses provide the oil and gas (O&G) industry with essential information and knowledge for the design and engineering of offshore installations, such as platforms and pipelines, and the adoption of decision support systems.

During the past decades, traditional measuring systems, such as wave buoys and wave radar systems, have been complemented by new technologies, examples of which are the vessel motion based wave inference techniques (VMBs).

The main benefits related to the adoption of VMB for the shipping industry as well as for the O&G industry have been discussed in several works, e.g. [14,15,18]. As a matter of fact, the VMBs can be adopted in applications that rely on real-time data, such as decision support systems for offshore operations as well as a complement to traditional measurement methods during wave data monitoring campaigns, since ships and offshore platforms can work together to provide worldwide information about the sea conditions, even from remote areas, at anytime. VMBs open up new possibilities for the assessment of the sea conditions, such as the use of wind turbine floating offshore platforms, likely to be installed in great number in forecoming years, as wave sensors.

Other potential applications for VMBs arise from the adoption of dynamic positioning systems and remotely-operated O&G floating systems (see e.g. Brodtkorb et al. [4]) that not only use real-time metocean data for a safety and effective operability but also to minimize the risks and impacts that failure scenarios (such as oil spills) may have onto the offshore and coastal environment and associated human activities.

This growing interest on the VMBs has been also motivated by the accuracy of the results obtained in different research works (see e.g. Nielsen [15], Iseki and Ohtsu [9], Bispo et al. [3] and Mak and Düz [11]) and by the fact that VMBs collect and process the necessary data to estimate the sea conditions by means of simple low-cost hardware that most of the O&G offshore platforms and shipping vessels have already installed on-board.

At the same time, there are some difficulties associated with measuring the wave conditions through VMBs. Indeed, different drawbacks may arise for certain sea conditions (usually extreme weather conditions when non-linear responses of the vessel become relevant).

* Corresponding author at: Naval Arch. & Ocean Eng. Department, Escola Politécnica da Universidade de São Paulo (USP), Brazil.
E-mail address: jordi.msoler@upm.es (J. Mas-Soler).

https://doi.org/10.1016/j.apor.2020.102125
Received 19 July 2019; Received in revised form 22 February 2020; Accepted 16 March 2020
Available online 30 April 2020

Therefore, in some sporadic cases, the conventional VMBs followed to evaluate the unknown sea conditions may result in misleading estimations of the wave spectrum (see [23]).

A preliminary assessment regarding the main impact that inaccurate estimations of the RAOs may have on the output of a parametric VMB is provided by Tannuri et al. [20]. The sensitive study carried out by the authors was based on the emulation of the inaccuracies of the RAOs in a VLCC by means of adopting erroneous draft conditions of the vessel. The results obtained attested that the outputs of VMB are linked to the accuracy of the RAOs and large errors in the estimation of the RAOs may lead to non-robust estimation of the sea states.

Iseki [8] aims at introducing the RAOs estimation inaccuracies in a Bayesian VMB by means of a RAO uncertainty matrix. For this purpose the values of the RAOs errors were assumed normally distributed with pre-defined values, which were adopted *ad hoc* to obtain accurate solutions. The accuracy of this very original approach proposed to take into account for the RAOs error in a Bayesian VMB was attested by the data obtained during a full scale experimental campaign. Notwithstanding this, the generality of the proposed approach can be challenged as a consequence of the methodology adopted to estimate the values of the RAOs errors.

The present work improves the procedure proposed in [8] by means of using the coherence functions of the motions to include, in the sea state computation, a correction accounting for the limitations of the linear modelling of the RAOs. The inference approach proposed has been adopted as the main mechanism to assess the possible effects that may arise when the nonlinearity related inaccuracies in the estimation of the RAOs are taken into account in the Bayesian VMB. This assessment is based on a comprehensive comparison between the results obtained using the proposed modified inference approach and the estimations drawn through the conventional Bayesian VMB, as adopted by Mas-Soler et al. [12].

The paper is organized as follows: Section 2 provides a description of the novel VMB able to account for the limitations of the linear modelling of the motion RAOs. The description of the semi-submersible unit adopted as a case study and the main features of the experimental campaign carried out at TPN-USP (wave basin of the University of São Paulo), have been included in Section 3. Section 4 is devoted to a comprehensive analysis of the RAOs inaccuracies and their impact on the performance of the Bayesian VMB. Concerning the main results, the outputs of the proposed VMB are compared with the results of the conventional one in Section 5, including an assessment of the estimations obtained for the wave statistics as well as a detailed analysis of the inferred sea spectra. Finally, the main conclusions drawn from this study are presented and discussed along with the possible further steps that should be taken in the continuity of this research.

2. Methodology

VMBs are based on the wave buoy analogy, which aim at solving the linear inverse problem of estimating the sea state given the measured motions and the transfer function of the platform. A common approach, see [13], adopted to infer the sea conditions is to assume a linear relation between the wave excitation forces and the vessel responses. Thus, the cross spectra of the motion time series can be formally expressed through the following identity,

$$\phi_{ij}(\omega) = \int_{-\pi}^{\pi} Z_i(\omega, \beta) Z_j^*(\omega, \beta) S(\omega, \beta) \mathrm{d}\beta \,, \tag{1}$$

where $Z_i(\omega, \beta)$ is the RAO of the ith motion at wave frequency ω and direction of incidence β, $Z_j^*(\omega, \beta)$ stands for the complex conjugate of the jth motion RAO, and $S(\omega, \beta)$ is the directional wave spectrum.

The relation given in Eq. (1) can be approximated in discrete form assuming the integrand to be constant in each slice $\Delta\beta = \frac{2\pi}{K}$. Thus,

$$\phi_{ij}(\omega) = \Delta\beta \sum_{k=1}^{K} Z_i(\omega, \beta_k) Z_j^*(\omega, \beta_k) S(\omega, \beta_k) \,. \tag{2}$$

where $\beta_k = -\pi + (k-1)\Delta\beta$ and K is the number of discrete wave directions considered. Concerning the indices i and j, they correspond to the N dofs (degrees of freedom) assessed.[1]

According to Iseki [8] and Tannuri et al. [20] the lack of an accurate characterization of the floating system, its loading conditions and the nonlinearity of the motions are among the most relevant effects that may lead to the misleading estimations of the RAOs. Aiming at accounting for nonlinearity type of inaccuracies, introduced by these and other effects, Eq. (2) can be rewritten following the proposal provided in [8],

$$\begin{aligned} \phi_{ij}(\omega) = \; & \Delta\beta \sum_{k=1}^{K} [(Z_i(\omega, \beta_k) + \delta_i(\omega, \beta_k)) \cdot \\ & (Z_j(\omega, \beta_k) + \delta_j(\omega, \beta_k))^* \cdot S(\omega, \beta_k)] \,, \end{aligned} \tag{3}$$

where $\delta_i(\omega, \beta_k)$ and $\delta_j(\omega, \beta_k)$ stand as the deviations associated to the estimations of the RAOs for the i and j dofs, respectively. Some authors, see for example Iseki [8] and Soares [19], adopt a statistical description of these deviations treating them as errors, which are assumed to be normally distributed with zero mean. The adoption of this approach has associated attractive simplifications from a practical point of view. Nonetheless, in [8], the author pointed out that the errors of the RAOs may be characterized for being non-normally distributed.

In the present study the deviations described above are not treated as errors related to the RAOs, as it has been done in previous works. This is possible since the RAOs are obtained through a comprehensive study with a well established numerical method. As a matter of fact, these deviations from the expected behaviour will be referred as nonlinearly related inaccuracies and referred as ε to highlight the inherent difference with the treatment adopted in previous works.

From the calculation of the measured motion spectrum it is observed that the cross-spectrum of motions i, j is Hermitian, i.e. $S_{ij} = \bar{S}_{ji}$, and, as a consequence, Eq. (3) can be rewritten in matrix form as follows,

$$\mathbf{B} = (\mathbf{A} + \mathbf{C})\mathbf{x} \,, \tag{4}$$

where the vector $\mathbf{B}$ contains a total of $(N^2 \cdot M \times 1)$ elements, which are related to the measured motion spectra, and M being the number of discrete frequencies. The RAO matrix is represented by the matrix $\mathbf{A}$, which is formed by a diagonal of M matrices, each one with $(N^2 \cdot M) \times (K \cdot M)$ elements. The vector $\mathbf{x}$ stands as the unknown sea spectrum, evaluated at the $(K \cdot M)$ pairs of directions and frequencies. For a comprehensive description of the quantities $\mathbf{B}$, $\mathbf{A}$ and $\mathbf{x}$, the reader is referred to [15].

Concerning matrix $\mathbf{C}$, it is given by the products of RAOS and their associated non-linearity related inaccuracies. Also, it presents the same dimensions as matrix $\mathbf{A}$. Iseki [8] adopts an heuristically constant predefined values for RAOs deviations (once again, referred as errors), δ. In this study, however, the values of the RAOs deviations have been computed by means of the coherence functions for each direction and frequency. The resulting non-linearity related inaccuracies, ε, of the RAOs for each frequency and direction pair can be estimated as follows (see [2]),

$$\varepsilon_i = \varepsilon(Z_i) = \frac{(1 - \gamma_i^2)^{0.5}}{\sqrt{2}\,|\gamma_i|} |Z_i| \,, \tag{5}$$

where γ_i stands as the coherence function for the ith dof of the platform, which provides a measurement of the causality between the incoming wave, η, and motion response, ξ, of the platform (assuming that it can

[1] It is not uncommon that only three ($N = 3$) dofs of the floating vessel are adopted in the VMB, namely heave, roll and pitch. In this case the indices i, j will vary between 3 and 5 following the normal numbering in seakeeping literature.

be modelled as a linear system). The output of the coherence function ranges between zero and one. Therefore, if η and ξ are uncorrelated the sample coherence converges to zero and, otherwise, values equal to one indicate linearity between the excitation and the response.

The coherence function between η and ξ for a certain frequency, f^*, is defined as follows,

$$\gamma_{\eta\xi}(f^*) = \frac{S_{\eta\xi}(f^*)S_{\xi\eta}(f^*)}{S_{\eta\eta}(f^*)S_{\xi\xi}(f^*)}, \tag{6}$$

where $S_{\eta\xi}(f^*)S_{\xi\eta}(f^*) = S_{\eta\xi}(f^*)S^*_{\eta\xi}(f^*) = |S_{\eta\xi}(f^*)|^2$. Thus,

$$\gamma_{\eta\xi}(f^*) = \frac{|S_{\eta\xi}(f^*)|^2}{S_{\eta\eta}(f^*)S_{\xi\xi}(f^*)}, \tag{7}$$

Eq. (5) provides a straightforward approach to qualitatively characterize the non-linearity related inaccuracies. However, this approach is dependent on the availability of experimental measurements of the dynamic responses of the system under study and, therefore, its feasibility may be limited to existence of previous experimental results. This drawback (usually relevant in preliminary studies) may be overcome through the adoption of non-linearly estimated RAOs to compute the coherence functions, although this may result in a higher computer power needs during the RAOs estimation process.

Returning to the description of the elements of matrix **C**, they are given by,

$$\begin{aligned} C_{ij}(\omega, \beta) = \; & \Delta\beta\,[Z_i(\omega, \beta)\varepsilon_j(\omega, \beta) + Z_j(\omega, \beta)\varepsilon_i(\omega, \beta) \\ & + \varepsilon_i(\omega, \beta)\varepsilon_j(\omega, \beta)]\,. \end{aligned} \tag{8}$$

Note that the values of **C** tend to zero as the coherence functions tend to unity. These results agree with the nature of the approach adopted to model the dynamics of the platform. Under this approach, when the coherence functions point to a purely linear response (value equal to 1), it is expected, from a theoretical point of view, that the RAOs stand as a reliable approach to accurately estimate the responses of the vessel under study.

The linear model provided by Eq. (4) properly takes into account the inaccuracies that may arise from the estimation of the RAOs. However, from the point of view of the VMB, this model must also include the uncertainties related to the measurement of the motions, which are usually carried out by means of an ordinary set of accelerometers connected to a consumer-level PC. A common approach, followed in the literature (see [9]) to take into account these measurement uncertainties, is the adoption of a linear stochastic regression model,

$$\mathbf{B} = (\mathbf{A} + \mathbf{C})\mathbf{x} + \boldsymbol{\varepsilon}', \tag{9}$$

being $\boldsymbol{\varepsilon}'$ a vector with $M \cdot N^2$ elements representing the measurement noise, which has been assumed to be Normally distributed, with zero mean value and variance $\sigma^2_{\varepsilon'}$.

A straightforward methodology to reconstruct the unknown sea spectrum from Eq. (9) would be the use of the inverse transform with the inverse filter, which is possible by using the pseudoinverse of matrix **A**. However, the nature of the problem[2] may lead to misleading estimations of the sea state. In order to properly infer the sea conditions that induced the measured motions, the adoption of regularization conditions is needed to give priority to solutions featured with certain desirable features. First, see for example [15], it is assumed that the sea spectrum must be smooth and continuous. These conditions can be formally expressed (in the frequency domain[3]) as,

$$S(\omega_i, \beta_k) = \frac{1}{2}(S(\omega_{i-1}, \beta_k) + S(\omega_{i+1}, \beta_k)) + \varepsilon_p\,, \tag{10}$$

where $S(\omega_i\ \beta_k)$ is the sea spectrum value that corresponds to the pair of i frequency and k direction. It is worth to highlight that, once again, the model provided in Eq. (9) has some associated uncertainties. To account for them, a Normally distributed noise, ε_p, with zero mean value and variance σ^2_p, has been adopted. It is possible to show, by means of Taylor series (see [22]), that this prior noise, ε_p, stands as an approximation of $\frac{\Delta\omega^2}{2} S''_{\eta\eta}(\omega_i, \beta_k)$. Intuitively, the standard deviation of $\boldsymbol{\varepsilon}_p$ determines how much the reconstructed function (unknown spectrum) departs from a line.

Since the absence of boundary conditions may result in the overestimation of the sea energy close to the limits of the domain ($\omega \times \beta$) assessed in our problem, some additional conditions are usually adopted. In direction domain, see once again [15], it is assumed that the following relation is fulfilled: $S(\omega_i, \beta_0) = S(\omega_i, \beta_K)$ and $S(\omega_i, \beta_{K+1}) = S(\omega_i, \beta_1)$. Concerning the frequency domain, the condition imposed is that the power of the spectrum goes to zero for $\omega \to 0$ and $\omega \to \infty$.

In addition, one must take care of another practical problem regarding the limitations due to the frequency insensitivity, i.e. wave frequencies for which part or all the motions of the platform are null. As a consequence, all the estimations in this frequency range are valid, and therefore uninformative of the actual ones. In order to avoid an overestimation of the spectrum energy leading to inconsistent results, the total energy of the spectrum is minimized in two pre-defined ranges of low and high frequencies.

These regularization conditions can be combined with the modified linear stochastic regression model by means of the Bayesian inference approach. As a matter of fact, its core principle is that the posterior distribution of the variable of interest is the result of updating the existing prior information on the model parameters using the available data, where the systematic process of learning from the data is implemented via Bayes theorem. This can be formally expressed as follows,

$$P(\mathbf{x}|\mathbf{B}) \propto P(\mathbf{B}|\mathbf{x})p(\mathbf{x})\,, \tag{11}$$

where $P(\mathbf{B}|\mathbf{x})$ is the posterior distribution, $P(\mathbf{B}|\mathbf{x})$ is the distribution of the measured data (i.e. the probability of observing the measured motions, **B**, given a sea state, **x**) and $p(\mathbf{x})$ stands as the prior distribution of observing the event **x**.

As the measurement noise in Eq. (9) is assumed Normally distributed with zero mean and variance σ^2, following [1], the probability distribution of the measured data can be written as,

$$P(\mathbf{B}|\mathbf{x}) \equiv \text{Const.} \times \exp\left(-\frac{1}{2\sigma^2}\,\|\mathbf{B} - (\mathbf{A} + \mathbf{C})\mathbf{x}\|^2\right), \tag{12}$$

Concerning the prior distribution, it can be deduced from the regularization conditions (i.e. the estimated sea condition must be smooth and continuous) adopted to properly estimate the sea state. Therefore, the prior distribution, as a direct consequence of the fact that the prior noise, ε_p, is Normally distributed with zero mean and variance σ^2_p, is given by,

$$p(\mathbf{x}) \equiv \text{Const.} \times \exp\left(-\frac{1}{2\sigma^2}[\mathbf{x}^T(u_1^2\mathbf{H}_1 + u_2^2\mathbf{H}_2 + u_3^2\mathbf{H}_3)\mathbf{x}]\right), \tag{13}$$

where u_1, u_2 and u_3 are known as hyperparameters and stand as the non-dimensional ratio between the variance of the measurement noise σ^2 and the variance of the prior distribution σ^2_p (for each one of the three regularization conditions adopted). Regarding the matrices $\mathbf{H}_1$, $\mathbf{H}_2$ and $\mathbf{H}_3$ they have been deduced from the regularization conditions described above (see Eq. (10)[4]).

[2] The resulting equation system is usually underdetermined and the pseudoinverse of matrix **A** is ill-conditioned.

[3] In direction domain this regularization condition is introduced by means of a similar expression.

[4] The reader is referred to [17] for a detailed description regarding the derivation of these regularization matrices.

Fig. 1. Åsgard-B semisubmersible floating gas production platform (left) and the 1:120 scaled semisubmersible platform model (right) (more detailed information is provided in [22]).

Table 1
General geometric properties of the semisubmersible platform and the model [22].

Properties	Full-scale	Small-scale
LOA (m)	102.4	0.853
B (m)	96.0	0.800
D (m)	45.0	0.375
Draft (m)	25.0	0.208
Width of pontoons (m)	19.20	0.16
Height of pontoons (m)	8.96	0.074
Diameter, corner columns (m)	19.20	0.16
Diameter, center columns (m)	12.20	0.10
Displacement	82700(t)	46.621(kg)
VCG (m)	33.28	0.27
GM_L (m)	3.32	0.028
GM_T (m)	3.31	0.028
Pitch inertia moment (kg · m^2)	$1.56 \cdot 10^{11}$	2.25
Roll inertia moment (kg · m^2)	$1.21 \cdot 10^{11}$	2.23
Heave natural period (s)	24	2.19
Pitch natural period (s)	88	8.03
Roll natural period (s)	74	6.75

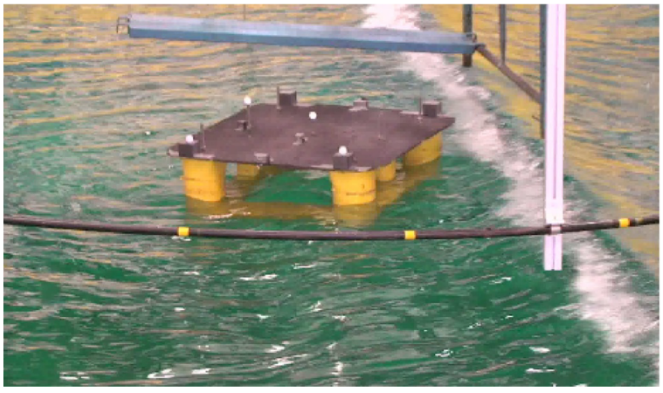

Fig. 2. Picture of the model-scale semisubmersible platform during one irregular wave condition at the TPN-USP.

Finally, combining Eqs. (12) and (13) by means of Eq. (11), the VMB problem of finding the unknown spectrum, $\mathbf{x}$, can be reduced to the minimization of the following functional,

$$J(\mathbf{x}) = \|\mathbf{B} - (\mathbf{A} + \mathbf{C})\mathbf{x}\|^2 + \mathbf{x}^T(u_1^2\mathbf{H}_1 + u_2^2\mathbf{H}_2 + u_3^2\mathbf{H}_3)\mathbf{x}. \quad (14)$$

which is feasible by means of a conventional quadratic algorithm. Note that to recover the conventional approach we merely need to disregard matrix $\mathbf{C}$ from Eq. (14).

3. Description of the experimental campaign

The experimental campaign was carried out in the TPN-USP wave basin using a scaled (1:120) model of the Equinor's Åsgard-B semisubmersible platform (see Fig. 1). The structure of the semisubmersible platform model is mainly composed by a rectangular ring pontoon connected to the deck by six box shaped columns. Concerning the main features of the real scale semisubmersible platform and the model, they are given in Table 1. The desired properties of the model were experimentally validated using bifilar pendulum tests, static inclination tests, decay tests and regular wave tests, which ensured a proper calibration of the mass-inertia properties of the model.

The experimental campaign comprised 32 different long-crested irregular sea conditions, ranging from mild waves with high probability of occurrence to extremal 100yr-return events, with a full-scale equivalent time duration of 1.5 hours[5], each. Moreover, aiming at increasing the reliability of the assessment of the VMB, two different sea spectra were adopted, namely Torsethaugen [21] and JONSWAP [7] sea spectrum. For a comprehensive description of the experimental campaign and the criteria followed to select the most convenient sea spectrum for each sea condition tested at the TPN-USP, the reader is referred to [12]. Aiming at providing a general idea of the waves generated during the experimental campaign Fig. 2 shows the semisubmersible platform during an irregular wave test.

The campaign comprised only one draft (operational) and five wave headings from bow waves to beam waves (in this case: 180°, 150°, 135°, 120° and 90°). Since one end of the tank acted as an actuator (generating the waves) and the other end was used as a wave-absorbing surface for all the sea condition tested, the correct heading conditions were guaranteed by means of changing the (relative) orientation of the model in the tank (always keeping the mooring characteristics unchanged). Finally, it is important to remember that during the tests, the motions of the model were recorded with an optical tracking system, that stands as a non-intrusive measurement system with linear displacement uncertainty equal to 0.1 mm.

4. Assessment of the numerical model

4.1. Comparison between the numerical and experimental RAOs

The dependence between the accuracy of the estimations obtained through VMB and the quality of the RAOs has been highlighted in Section 2. Tannuri et al. [20] showed that the main inaccuracies concerning the conventional numerically estimated RAOs are due to the following factors: (i) Non-linearities, that may become relevant for motions that are strongly dependent on viscous forces as well as when the vessel response amplitudes reach high values, and (ii) load conditions inaccuracies, due to the fact that the vessel response depends on its load distribution.

In this work, the hydrodynamic coefficients and RAOs adopted (i.e. heave, roll and pitch) to estimate the sea conditions were computed by

[5] The time series of the sea conditions can be assumed stationary within the time span assessed during the tests (see [12]).

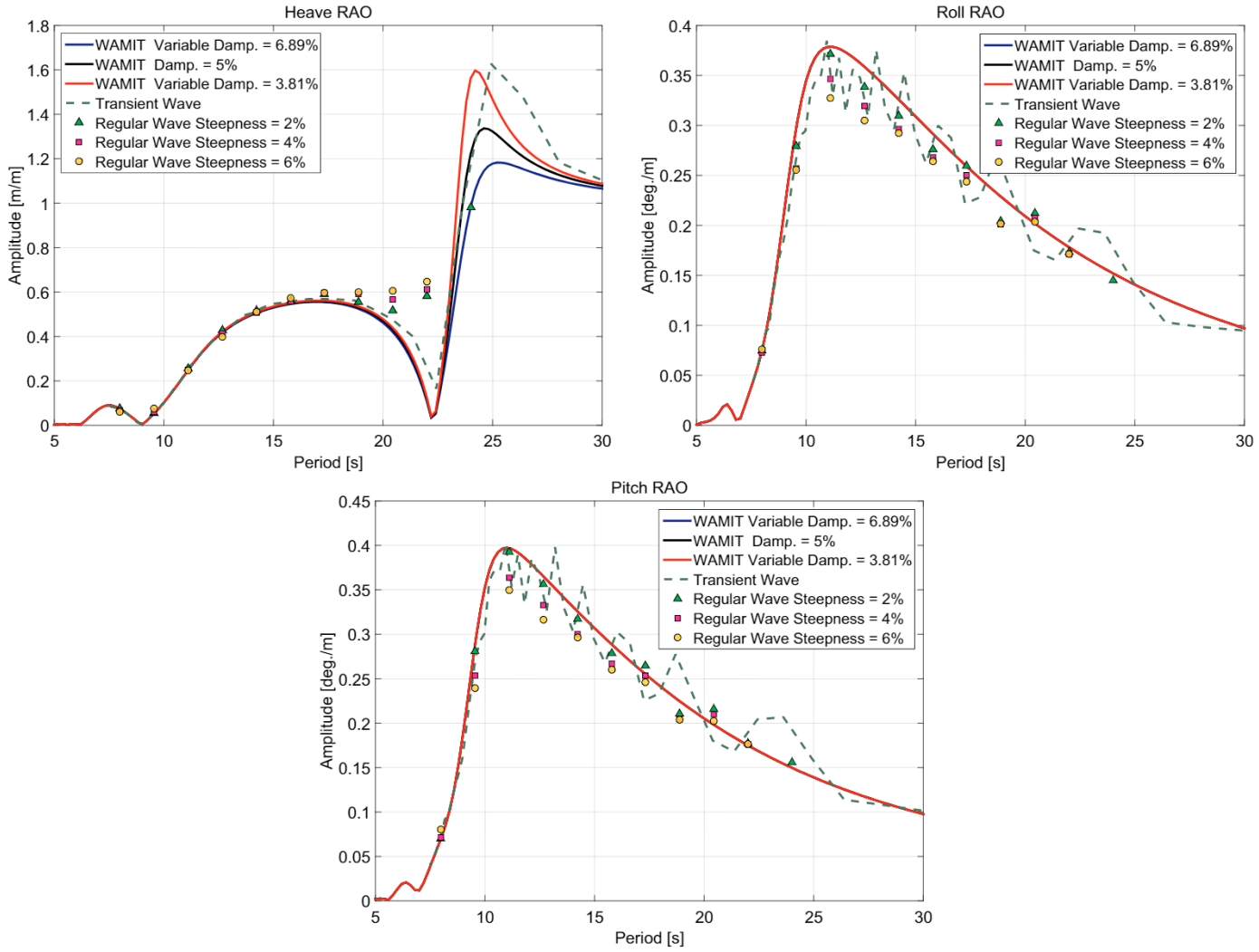

Fig. 3. Comparison of the (heave, roll and pitch) RAOs estimated numerically (black, blue and red lines) with the experimental results both transient (green dashed line) and regular waves with 2%, 4% and 6% steepnesses (colored markers). (For interpretation of the references to colour in this figure legend, the reader is referred to the web version of this article.)

means of the software WAMIT [10]. However, as a direct consequence of the small potential damping coefficients that characterize the semi-submersible platforms, non-linear viscous effects may be particularly relevant close to the heave motion resonance, which occur inside the frequency range of interest. Such effects are not modeled by the numerical method adopted for computing the RAOs, which is based on potential flow and assumes a linear dynamic response. In order to avoid an excessive loss of accuracy using the VMB, a simple estimation of the external damping was obtained following the proposal derived in [12], with damping ratio, ζ, of the heave motion being estimated as,

$$\zeta = \frac{b_1 + b_2^{\text{Equiv}}}{b_{\text{crit}}} \underset{b_1 << b_2^{\text{Equiv}}}{\rightarrow} \zeta \approx \frac{b_2^{\text{Equiv}}}{b_{\text{crit}}} = \frac{b_2^{\text{Equiv}}}{2\,\omega_n\,(M + a_{33})} = \frac{2}{3\pi}\rho\, C_d\, A_z \frac{l_{\text{pont}}\,(h_{\text{pont}}\,b_{\text{pont}})}{(M + a_{33})}, \tag{15}$$

where b_1 is the linear damping coefficient and b_2^{Equiv} stands as a linearization of the quadratic damping coefficient. h_{pont} and b_{pont} represent the height and the beam of the pontoons, respectively. l_{pont} is the length of the pontoons in-between columns, C_d the cross-sectional drag coefficient of the pontoon, a_{33} the heave added mass for the heave natural frequency, M the total mass of the platform and ρ is the seawater density. Regarding A_z, it stands as a representative amplitude of the heave motion, and has been computed as,

$$A_z = \sqrt{2 S_{zz}(\omega_n) \cdot \delta\omega_n}\,, \tag{16}$$

where $S_{zz}(\omega_n)$ is the measured power spectrum of the heave motion at the natural frequency and $\delta\omega_n$ is the frequency interval of the spectral analysis close to the natural frequency (ω_n), or $\delta\omega_n = \omega_{(n+1)} - \omega_{(n-1)}$.

Since the measured power spectrum of the heave motion is known from the records of motions of the platform, Eq. (15) allows the estimation of ζ for each case.

It is important to keep in mind that novel theoretical and numerical approaches, such as the one adopted in [16], may account for the different non-linear forces with no need of linearization. Therefore, increasing the accuracy of the estimated response functions of the system under study. The complexity and computational expense, however, are still nowadays as one of the major perceived barriers to the use of these techniques.

Regarding the second main cause that may lead to inaccurate RAOs estimations, the semisubmersible platforms are characterized by a small value of the metacentric height (GM), which limits its stability properties. As a consequence, these platforms constantly monitor their GM values. This feature turns to be an advantage for the semisubmersible platforms to be used as motion based wave sensors, since they allow the estimation of the most appropriate set of RAOs at any time. This fact makes them different to other vessels and offshore platforms, such as the FPSOs, which present large draft variations that result in the

increase of the RAOs inaccuracies as a direct consequence of the significant changes of their stability properties, i.e. their GM and the position of their centre of gravity. This limitation regarding the use of the FPSO as VMB wave sensor is well illustrated in [3], where the authors carried out a sensitivity study to assess the RAOs changes of a FPSO in different loading conditions.

Coming back to present research, the level of agreement between the motion RAOs obtained from the wave tests (both for transient[6] and regular waves) and those computed numerically is illustrated in Fig. 3. The results provided correspond to a platform heading of 135deg. and comprise only the three motions that were used for the purpose of wave inference (heave, roll, pitch). Due to the technical limitations of the wave basin, the estimations of the RAOs estimated by means of the regular waves with 4% and 6% steepnesses are limited to a maximum period equal to 22 s.[7]

First, the heave motion RAOs are provided. They were computed with $\zeta = 5\%$ as well as with $\zeta = 3.81\%$ and $\zeta = 6.89\%$. The damping values 3.81% and 6.89% were estimated through Eq. (15) and correspond to the amplitudes deduced from the transient wave and the regular wave with steepness equal to 2%, respectively. In general, numerical and experimental results show good agreement. However, the results provided also attest that significant differences in the vertical motions of the platform may appear due to viscous effects for high wave periods. These effects include, along with the attenuation of the resonant amplification, the suppression of the cancellation point of the RAO. The later effect results from the velocity dependent drag forces and, therefore, it cannot be reproduced by merely adding an external damping coefficient to the analysis carried out in the frequency domain.

Secondly, the RAOs of the angular motions, also provided in Fig. 3, show that the numerical estimated RAOs follow the tendency of the experimental points but lie slightly above them. It is important to keep in mind that in this case the numerical computations obtained with the different external damping coefficients drawn the same estimations of the angular RAOs, since their natural frequencies are equal to 74 and 88 seconds, respectively.

Observation of the results provided in Fig. 3 suggests that a quantitative assessment of the accuracy of the numerically estimated RAOs can be carried out by means of a model for the deviations of the RAOs with respect to the experimental ones. It should be noticed that a model using a constant value (in both frequency and direction) for the deviations can be an adequate approach to assess the accuracy of the RAOs evaluated in the present work, due to the fact that the differences between experimental and numerical results are in general not large. Moreover, as the data available is limited, it is natural to adopt the simplest idealization. Therefore, the model adopted for this assessment can be expressed as follows,

$$\hat{Z} = \alpha \cdot Z + \varepsilon \,, \tag{17}$$

where $\hat{Z}$ is the measured values of the RAO, Z represents the RAO numerical predictions and ε stands as the experimental stochastic deviation, which is assumed to be featured with a zero mean. Since this representation assumes that the measurement errors are independent of the frequency. The value of the constant α can be estimated by a direct minimization of the sum of the squares of the errors.

The estimations of the expected value of the constant, α, have been obtained using the transfer function computed numerically and those obtained experimentally through the regular waves. Furthermore, the narrow differences between the experimental results obtained by means of three different steepnesses allow the computation of the least squares adopting the results as different realization of the same process. Thus, the objective function for each motion is given by:

$$\hat{Z}_{ij} = \alpha \cdot Z_i + \varepsilon_{ij} \,. \tag{18}$$

where $\hat{Z}_{ij}$ is the measurement of the transfer function corresponding to the ith frequency and the jth regular wave. As a result, for each one of the 11 different frequencies tested using the regular waves, there are three measurements (i.e. $j = 1, 2, 3$), which stand for the steepnesses equal to 2%, 4% and 6%.

Table 2 provides the values obtained for α, by means of minimizing the following sum of the squares of the errors,

$$L = \sum_i \sum_j \varepsilon_{ij}^2 = \sum_i \sum_j (H_{ij} - \alpha \cdot H_i)^2 \,. \tag{19}$$

The results in Table 2 show a tendency of the numerical RAOs to slightly overestimate the rotational responses of the platform under study. Nonetheless, the estimated values for the constant α are almost equal to one in all the directions assessed and, consequently, the differences between the experimental results and the numerical ones can be assumed negligible.

Concerning the responses of the heave motions, the numerically computed RAOs underestimate the measured motions with constant errors that are close to 20%. The observed discrepancies are a direct consequence of the suppression of the cancellation point of the heave RAO due to non-linear effects, which are velocity dependent and, therefore, they cannot be reproduced through the analysis carried out in the frequency domain.

4.2. Consistency of the VMB model

In order to assess the impact of the RAOs inaccuracies on the consistency of the VMB in a simple manner, this section provides a comparison of the norms of the differences between the measured motions and the estimated ones by means of the numerically computed RAOs (see Eq. (20)) and the norms of the differences between the measured motions and the expected ones if the RAOs inaccuracies are taken into account (see Eq. (21)).

$$N_1 = \|\mathbf{B} - \mathbf{A}\mathbf{x}\|^2 \,, \tag{20}$$

$$N_2 = \|\mathbf{B} - (\mathbf{A} + \mathbf{C})\mathbf{x}\|^2 \,. \tag{21}$$

Fig. 4 shows the comparison of the results obtained through Eq. (20) (rhombus markers) and (21) (square markers), for all the 32 different sea conditions and five headings tested during the experimental campaign. In order to provide an effective comparison of the outputs, the results have been sorted according to the mean wave period (T_1). Furthermore, it is important to highlight that the norm values have been divided by the (measured) variance (m_0) of the corresponding sea condition. This normalization allows a meaningful comparison of the outputs, which are related to the energy that each sea state presents.

Regarding the quality of the estimations of the platform responses, Fig. 4 shows that the sea conditions characterized by large peak periods render the largest differences between the expected responses of the platform and the measured ones. These results are in agreement with the theoretical framework, since the non-linear drag effects become more relevant close to the resonance of the heave motion.

Overall, it is possible to state that the results in Fig. 4 attest

Table 2
Values obtained for α, according to the heading direction and response motions assessed.

	Heading (deg)				
Motion	90	120	135	150	180
Heave	1.17	1.17	1.18	1.20	1.20
Roll	0.96	0.93	0.93	0.91	–
Pitch	–	0.94	0.95	0.94	0.95

[6] The reader is referred to [5] for a comprehensive description of the main characteristics of a transient wave.

[7] The reader is referred to Table A.4 in Appendix A for a comprehensive description of the regular waves input parameters.

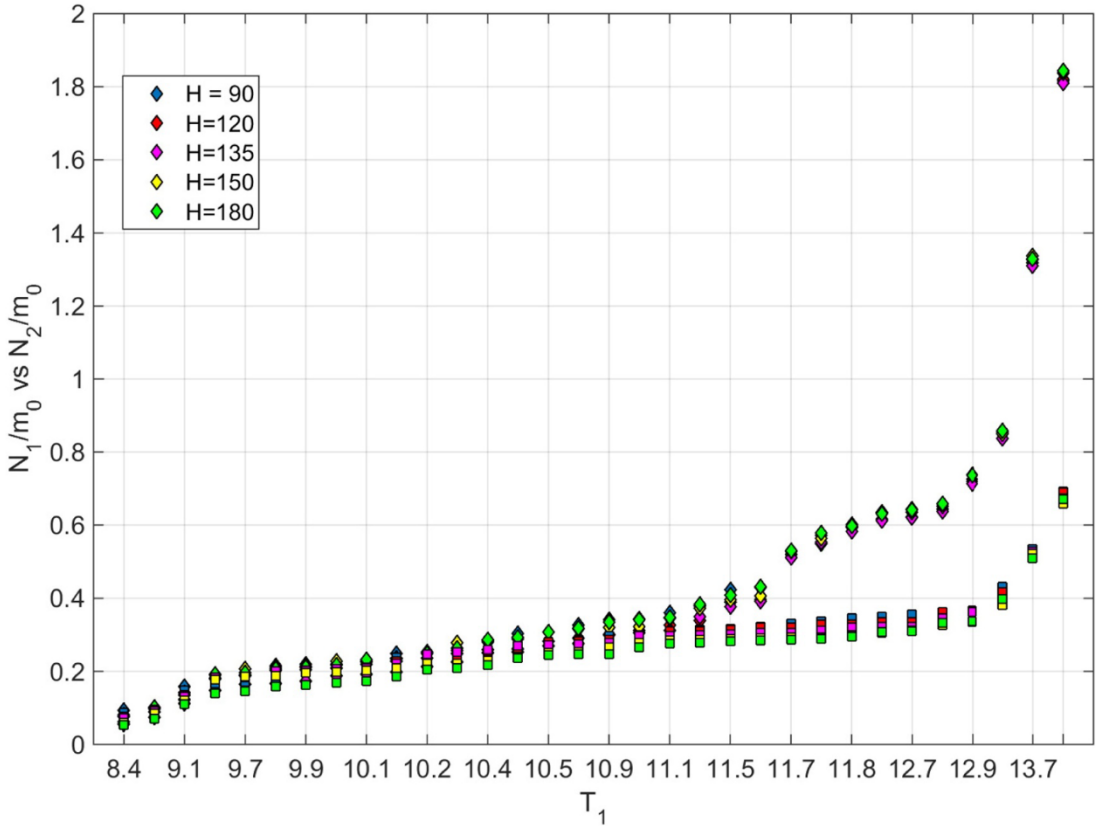

Fig. 4. Comparison between the norms of the differences of the measured motions and the estimated ones, including (square markers) and non-including (rhombus markers) of the RAOs inaccuracies.

significant improvements when the RAOs inaccuracies are taken into account to compute the norm (i.e. Eq. (21)). As a matter of fact, these improvements become more relevant for sea conditions featured with large peak periods than those with short peak periods, due to the impact of non-linear drag effects in this frequency range. These differences are in agreement with the observations provided in [12], where the authors pointed out that the semisubmersible platforms can be adopted as reliable VMB sensors even for sea conditions characterized with short peak periods.

Returning to the RAOs inaccuracies, we must keep in mind that the values of the norm in Eq. (20) will tend to zero if the proper experimental RAO is adopted as the dynamic model of the platform and, therefore, increasing the accuracy of the estimations of the sea conditions. Notwithstanding this, the observed reduction of the differences between the measured motions and the expected ones, when taking into account the RAOs inaccuracies, attests the accuracy of the proposed VMB.

5. Results

In the following, the effectiveness of the modified Bayesian approach discussed in Section 2 has been assessed by means of a comprehensive comparison against the conventional approach, as provided by Mas-Soler et al. [12].

Regarding the values of the hyperparameters, their optimal values were determined by means of an extensive sensitivity analysis. Thus, it was determined that: u_1 and u_2 are equal to 0.0035 and $1{\cdot}10^{-5}$, respectively. These values are the same ones adopted in [12]. Nonetheless, u_3 was set equal to $1{\cdot}10^{-7}$. The value adopted for the third hyperparameter stands as a direct consequence of the adoption of matrix **C**. As a matter of fact, the use of this error matrix avoids the over estimation of the sea energy when the platform presents non-linear response amplitudes and, therefore, larger values of u_3 (if compared with the values adopted in [3] and [12]) are no longer needed.

First, the quality of the estimations has been checked considering the main statistical parameters of the sea states, i.e. the mean wave period (T_1), significant wave height (H_s) and mean wave direction (θ). Aiming at providing an effective and proper visual formatting for the comparison of the results, the following arrangement is adopted: A representation of the distribution of the ratio between the value of the estimation and the measured value, for all the heading conditions (H = 90, 120, 135, 150, 180), in terms of box-plots. The sea wave statistics H_{s_m}, T_{1_m} and θ_m stand for the significant wave height, mean wave period and mean wave direction obtained from the measurements in the basin using a set of conventional wave probes. Returning to the box-plots in Figs. 5–7, they have been estimated using a nonparametric representation of the probability of the estimations obtained with different heading for each statistic assessed in this work (i.e. H_s, T_1 and θ_m). In this study, the box-plots report the following quantities for each sea condition tested:

1. The lower and upper limit of each box indicate the 25% and 75% percentile levels;
2. The central mark indicates the 50% percentile level;
3. The bars indicate the estimated 5% and 95% percentile levels while the remaining data-points outside of these limits are likely outliers.

Moreover, the results have been clustered into two different sets with different colors, indicating whether the waves generated in the basin corresponded to a JONSWAP (blue) or Torsethaugen (red) power spectrum. This approach allows a proper comparison between the results obtained with different headings.

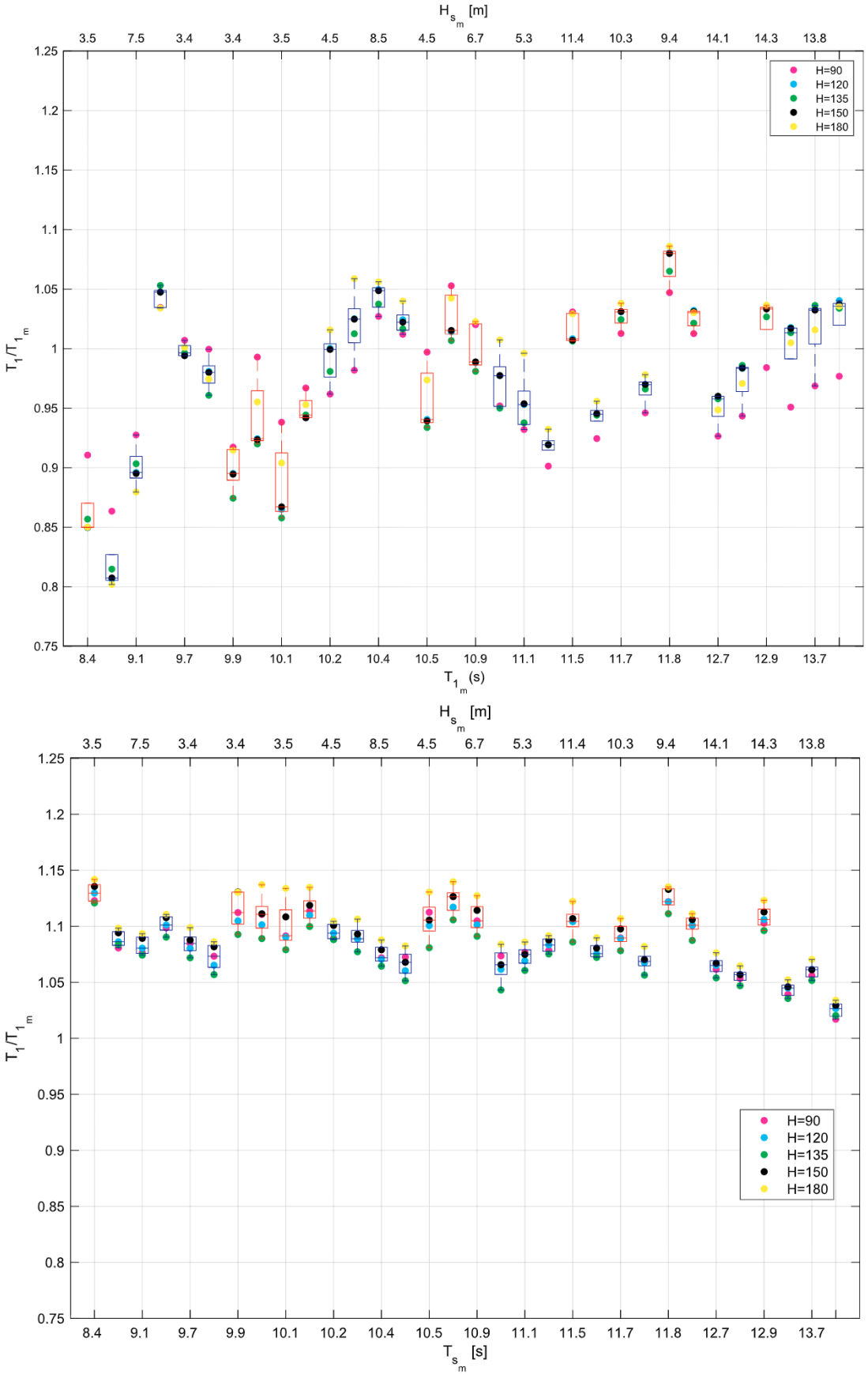

Fig. 5. Ratio between the estimated and measured mean wave period. Modified (top) and conventional (bottom) approaches.

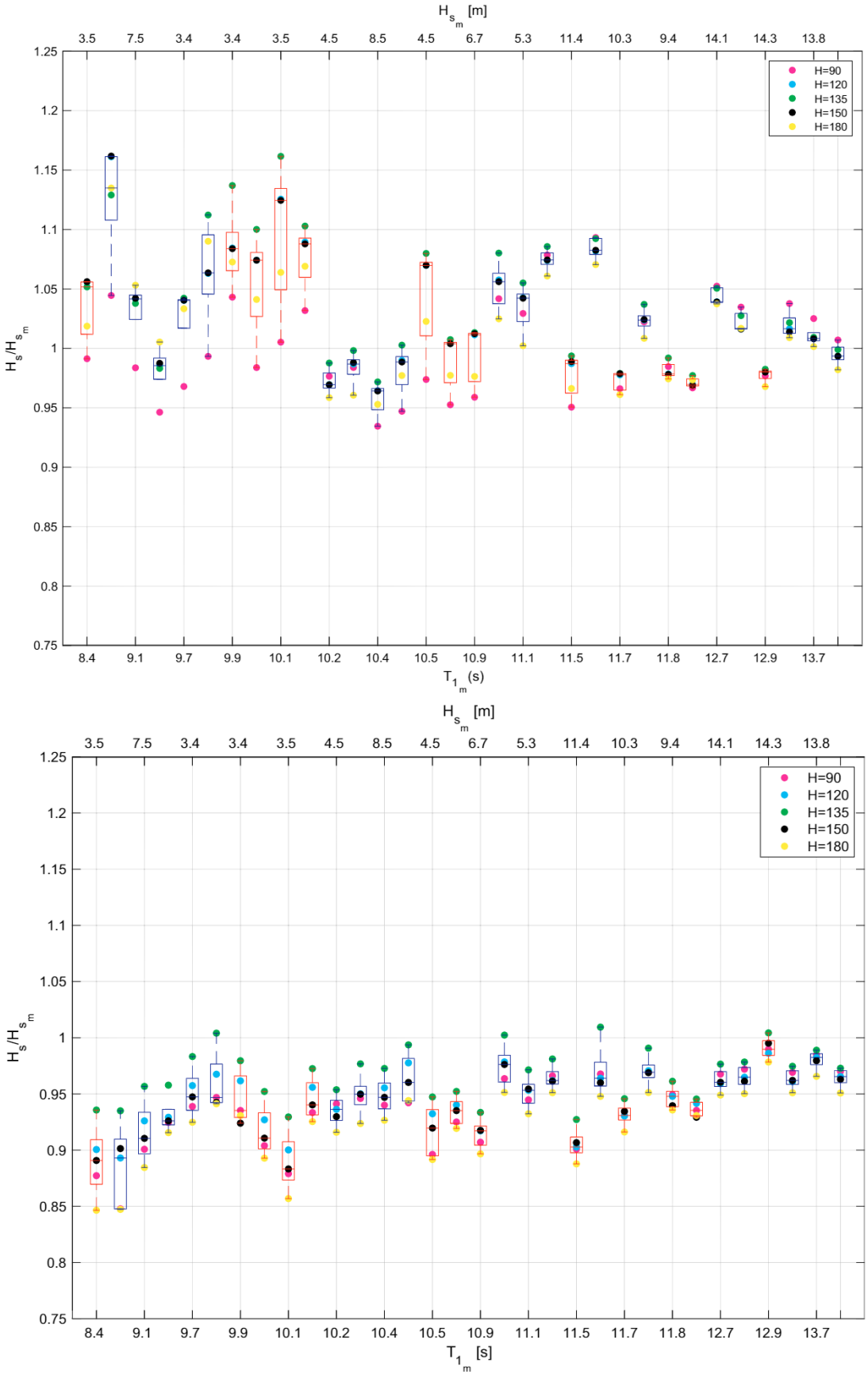

Fig. 6. Ratio between the estimated and measured significant wave height. Modified (top) and conventional (bottom) approaches.

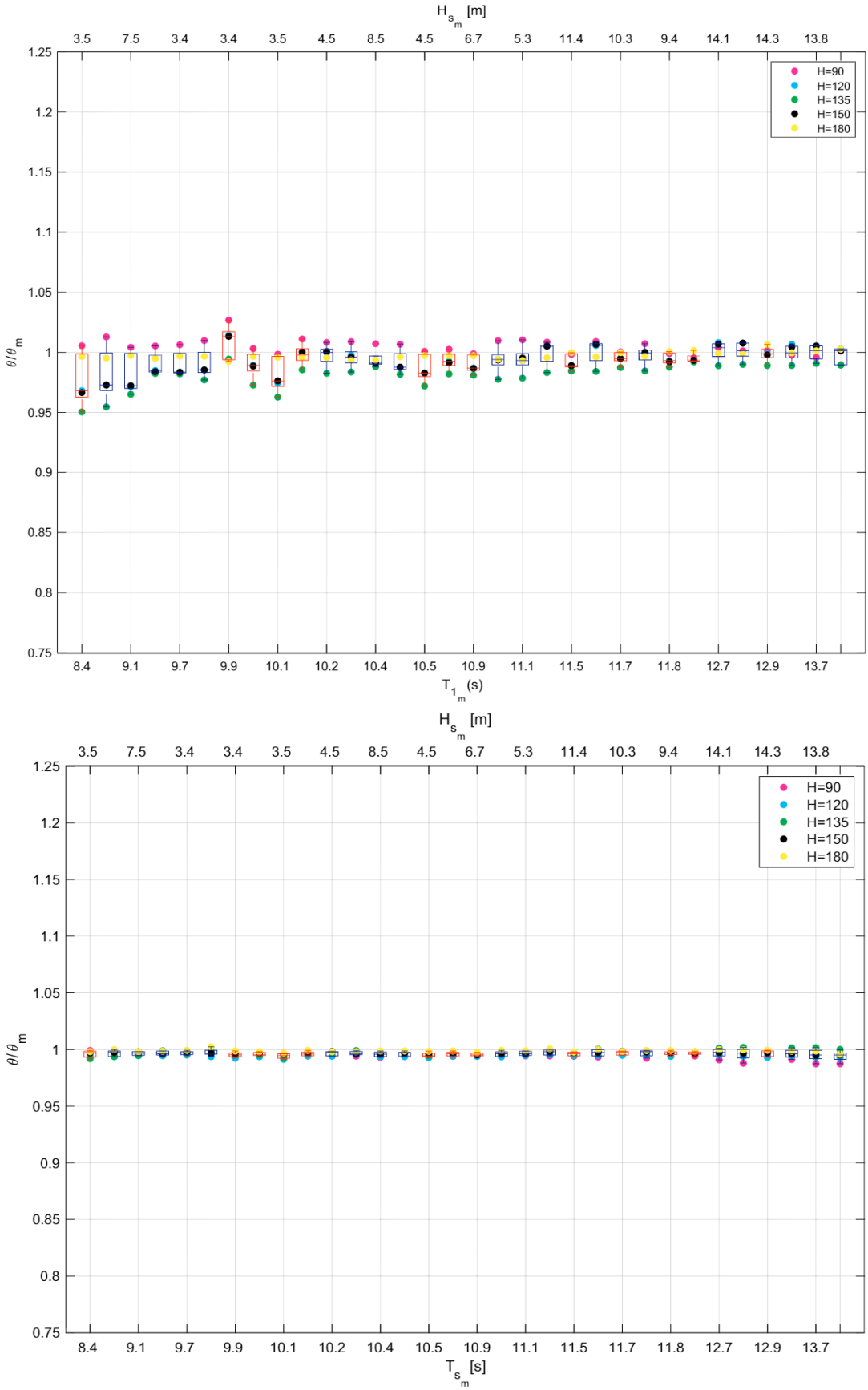

Fig. 7. Ratio between the estimated and measured mean wave direction. Modified (top) and conventional (bottom) approaches.

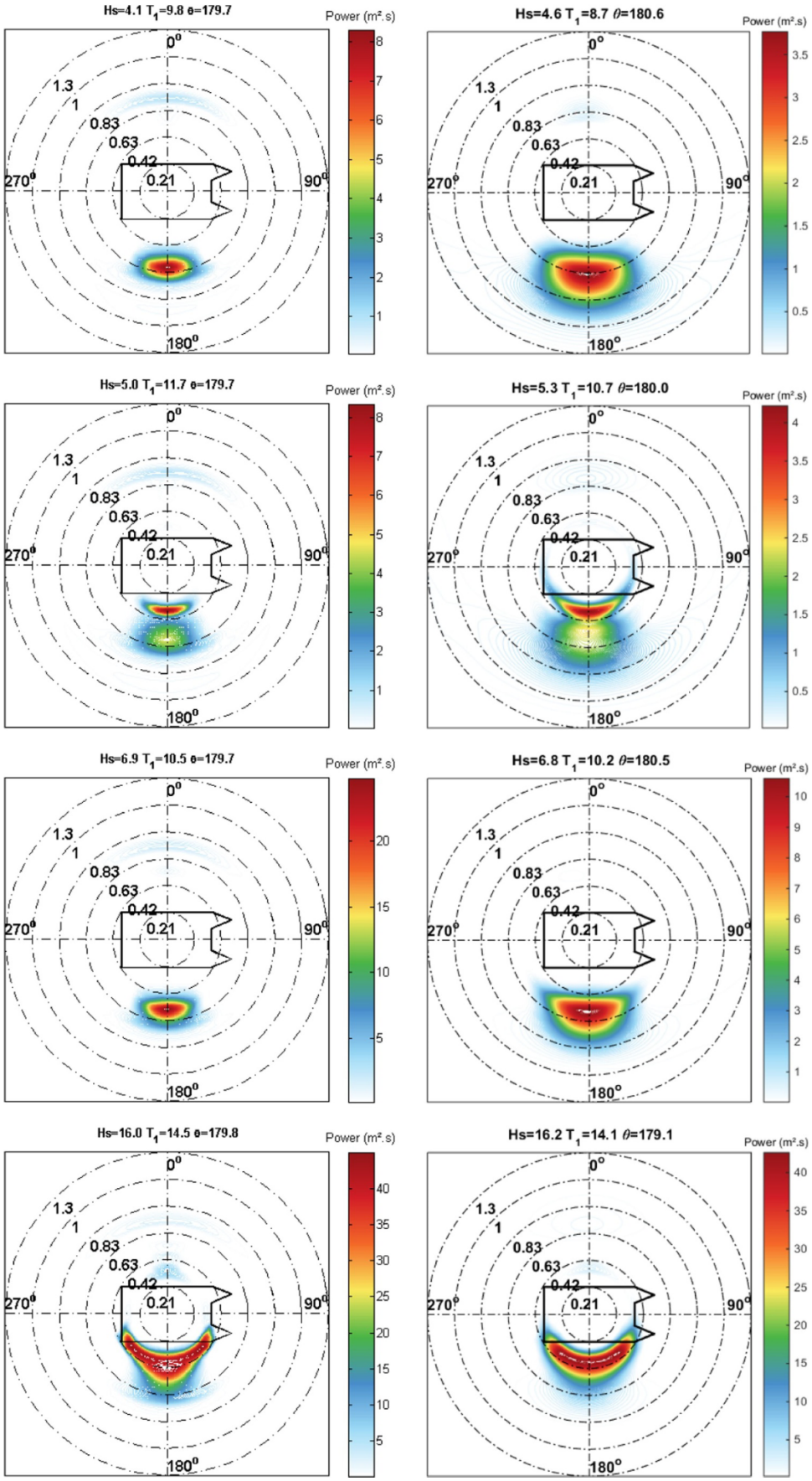

Fig. 8. Estimated wave spectra (from top-to-the-bottom) of the sea conditions in Table 3 and heading 90°. The left column stands as the estimation obtained by means of the conventional approach and the right column provides the outputs of the modified approach.

Table 3
Expected properties of the measured sea conditions (see [12]).

Test	Spectrum Type	H_{s_m}	T_{1_m}	Direction
6	JONSWAP	4.53	9.06	90/135°
12	Torsethaugen	5.54	10.48	90/135°
15	JONSWAP	7.50	9.60	90/135°
30	JONSWAP	16.21	13.73	90/135°

Figs. 5–7 attest that for sea conditions with measured mean wave periods larger than 10.1 s, the approach taking into account the RAOs inaccuracies provides improved estimations for both H_s and T_1 if compared with the ones reported in [12]. This tendency is well illustrated by the fact that the estimations obtained with the proposed approach for mild to extreme sea conditions are characterized with errors always below 10% for both the mean wave period and significant wave height, respectively, while the conventional approach resulted in estimations characterized with errors below 14% and 12%, once again, for the estimations of H_s and T_1. Notwithstanding this, it is important to highlight that the outputs of the proposed approach are characterized with larger spreading of the estimation according to the different headings assessed. This is mainly a direct result of the fact that the inaccuracies regarding the heave RAO are different, in the frequency and direction domain, when compared with the errors estimated for the roll and pitch motions, which result in similar error distributions (see Table 2).

Concerning the estimations of the milder sea conditions (mean wave periods lower than 10.1 s), the modified approach results in an overestimation of the significant wave height, with larger errors than the ones obtained by means of the conventional approach. This can be explained by the fact that these sea states present large amounts of energy in the frequency range where the platform responses are expected to be small, therefore associated to the increase of the inaccuracies of the RAOs and resulting in slightly lager errors on the estimation of the of sea wave energy distribution.

In a similar way, the estimations of the mean wave direction present the same pattern regarding the differences that arise between the outputs obtained with the heading conditions tested. Concerning the estimations of the directional sea spectra, Figs. 8 and 9 show the estimated directional sea spectra for wave conditions listed in Table 3. The colorbar in these figures represents the power spectral density. The direction (deg.) and frequency (rad.s^{-1}) are provided by the angular and radial direction dimensions of the sea spectrum, respectively.

The sea conditions described in Table 3 were selected among the 32 tests carried out during the experimental campaign in order to provide a representative sample of the whole range of periods that was tested, and their main characteristics (H_s and T_1) correspond to the measurements obtained by means of conventional wave probes.

Regarding the directional spectra included in Figs. 8 and 9, the wave energy in each wave frequency (radial coordinate in rad/s, with values given at full scale) is depicted for all wave directions (as a convention, the actual wave direction in the tank was considered as 180°). In addition, the main statistical parameters for each wave condition are presented at the top of each figure.

The results obtained show that the energy spreading in the direction domain (the directional resolution considered in this study is equal to $\Delta\theta = 5$) is larger for the estimations obtained with the modified approach than those obtained by means of the conventional inference technique. However, the waves generated at the wave basin were long-crested and, therefore, the obtained results with the conventional approach are in better agreement with the expected dispersion of the energy than the ones obtained taking into account the RAOs inaccuracies.

The differences are a direct result of the adoption of the estimated inaccuracies of the RAOs, which are always larger than zero and, as a consequence, they force the method to spread the energy in order to minimize the error between the measured motions of the platform and the estimations. Furthermore, it is worth to remember that since the first and second hyperparameters are maintained unchanged in the modified approach, the effect that they may have on the energy spreading is the same in all the results provided. The authors hypothesize that the modified VMB may provide improved (i.e. better estimations than the conventional VMB) for short-crested sea conditions. As a matter of fact, the tested sea conditions tested stand as a limiting case for the wave inference problem to be solved and, furthermore, the modified VMB provides estimations of the sea spectra with large energy spreading (which can be explained by the non-zero inaccuracies introduced by the method in all the frequency-direction pairs). Therefore, the inference of short-crested sea conditions may lead to improved result for the developed VMB, since the spreading of the energy will be smaller than for long-crested sea states and it may result in better estimations of the total energy of the sea spectra.

Figs. 10 and 11 show the energy spectrum in frequency-domain for the sea conditions previously assessed in Figs. 8 and 9 (see Table 3). These figures include the wave spectra estimated using the conventional approach (dashed blue line) and the estimations obtained by means of the modified proposal (red dashed-dot line). Also, aiming at providing a reference for the estimations obtained, the sea spectra obtained from the wave probes records are included in these figures (black continuous lines).

From the results obtained concerning the sea spectrum in frequency-domain, one may realize that the modified approach outputs less accurate results than the conventional ones for mild sea conditions (i.e. test# 6), in both heading conditions evaluated.

Regarding the estimation obtained for the Torsethaugen sea conditions, the use of the proposed approach resulted in an improvement of the estimated energy distribution, even close to the cancelation points. As a matter of fact, the estimations obtained of test# 06 , 12 and 15 through the conventional approach in beam sea conditions show a significant discrepancy (close to 0.13Hz) between the measured wave spectra and the estimations. These differences can be linked to the points of minimum response that the roll and pitch RAOs present close to 7.5 s (see Fig. 3).

The extreme sea conditions evaluated in Figs. 10 and 11 have been estimated quite accurately using both approaches (conventional & modified). This is because the platform motions are characterized by larger amplitudes and, as a consequence, the errors for the estimations obtained of the directional sea spectra are lower than the ones obtained for mild sea conditions. This is in agreement with the results shown in Figs. 5 to 7 and in Section 4.2, which show a clear improvement of the estimations for the wave conditions that correspond to the extreme sea events.

Finally, it is important to highlight that the estimations obtained by means of the modified approach in all the cases have underestimated the energy close to the peaks of the wave spectra. This is a direct result, as it has been pointed out previously in this section, of the adoptions of the RAOs inaccuracies, which always present values larger than zero.

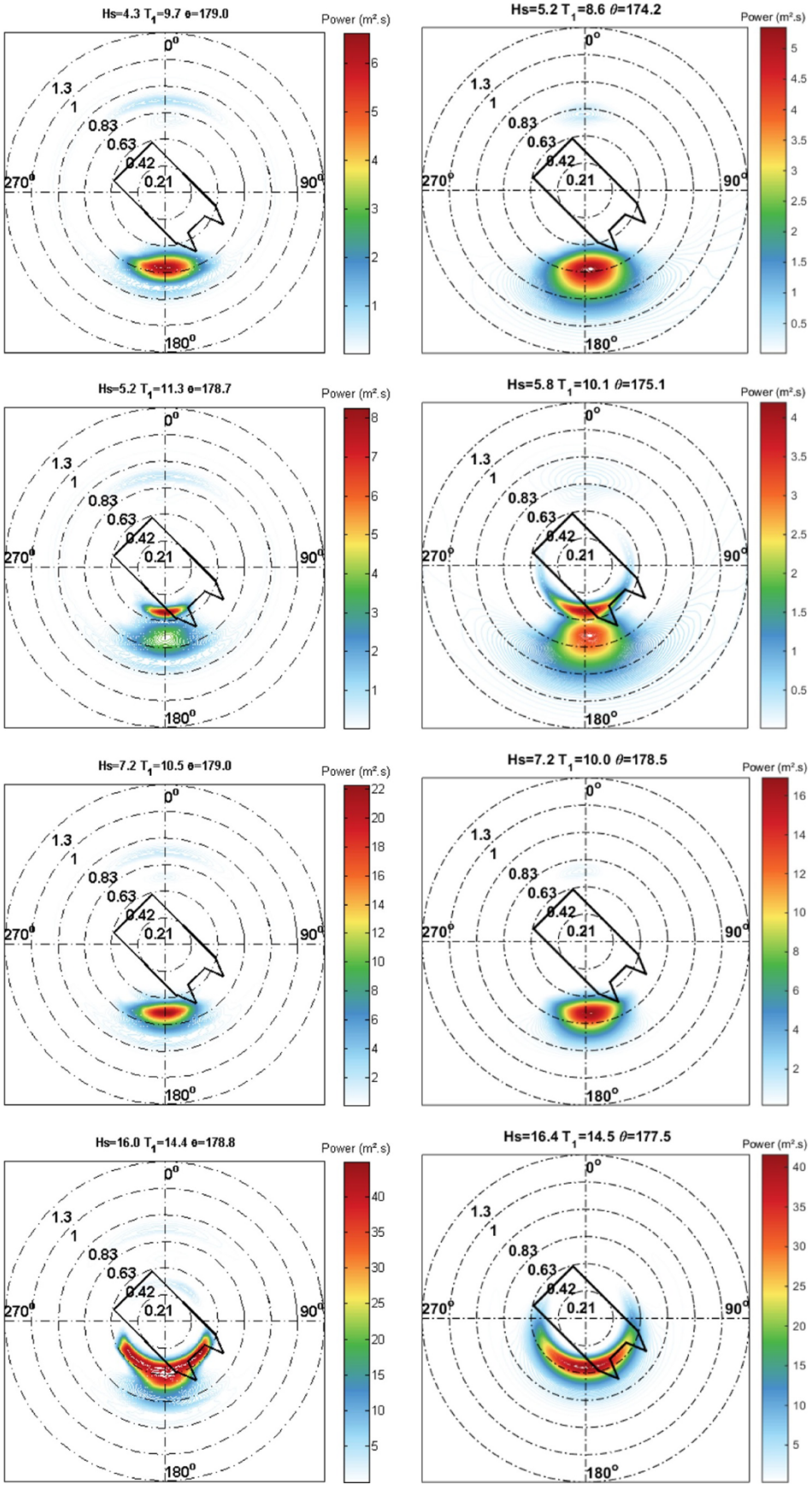

Fig. 9. Estimated wave spectra (from top-to-the-bottom) of the sea conditions in Table 3 and heading 135°. The left column stands as the estimation obtained by means of the conventional approach and the right column provides the outputs of the modified approach.

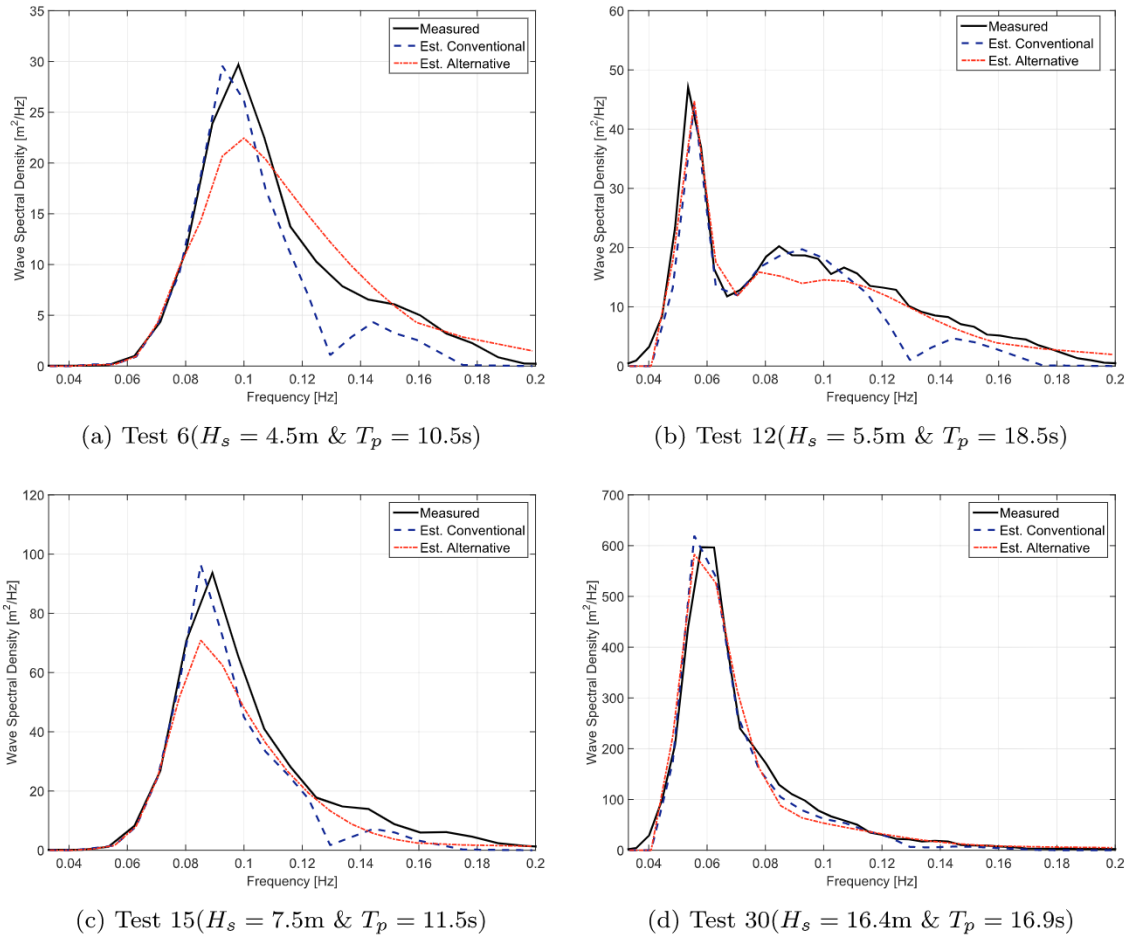

(a) Test 6($H_s = 4.5$m & $T_p = 10.5$s) (b) Test 12($H_s = 5.5$m & $T_p = 18.5$s)

(c) Test 15($H_s = 7.5$m & $T_p = 11.5$s) (d) Test 30($H_s = 16.4$m & $T_p = 16.9$s)

Fig. 10. 2D estimated sea spectra for heading 90°.

Thus, it is expected that the amount of energy close to the peak of the spectrum will be smaller than the measured one.

6. Conclusions

This work has provided a general assessment of the effects that nonlinearity related inaccuracies on the estimations of the RAOs may induce on the outputs of the Vessel Motion Based wave inference approach (VMB). For this purpose an improved Bayesian VMB, which takes into account the limitations of the linear modelling the RAOs, has been developed. The improvements of the proposed methodology have been assessed by means of a comprehensive comparison against the estimations obtained with the conventional approach, using the data from a controlled model scale experimental campaign with the Equinor's Åsgard-B semsisubmersible platform, that was carried out at the TPN-USP.

The comparison has shown that the proposed VMB approach may lead, in some sea conditions, to the improvement of the estimations, specially those that correspond to mild to extreme sea states. This improvement is in agreement with the one observed regarding the consistency of the VMB for those sea conditions featured with large peak periods, if the RAOs inaccuracies are included in the platform motion model.

On the negative side, the adoption of the modified VMB to take into account the RAOs nonlinearity related inaccuracies results for the Åsgard-B floater in directional estimations of the sea spectrum characterized by a larger energy spreading, both in frequency and direction domain, than the conventional one. However, the experimental campaign only included long crested sea conditions, which stand as a limiting case for the prior beliefs introduced in the inference problem (i.e. that the inferred directional sea spectrum must be smooth both in frequency and direction). As a matter of fact, the use of short crested sea states may result in the improvement of the directional sea spectra estimations if the proposed VMB is adopted. Investigating this matter has been left for future work.

Another drawback of the developed approach is its dependence on previous existing experimental results to compute the coherence functions. Although this shortcoming can be overcome by means of using non-linear methods to estimate the responses of the platform under certain conditions, such as time domain simulations. This alternative approach, however, may result in an increase of the computer power needs and total computing time. The assessment of the feasibility (in time and computer power costs) of these alternatives have been left as a thread of future work.

Together with better estimations in mild and extreme seas, a further advantage of the novel proposed method is the improvement of the

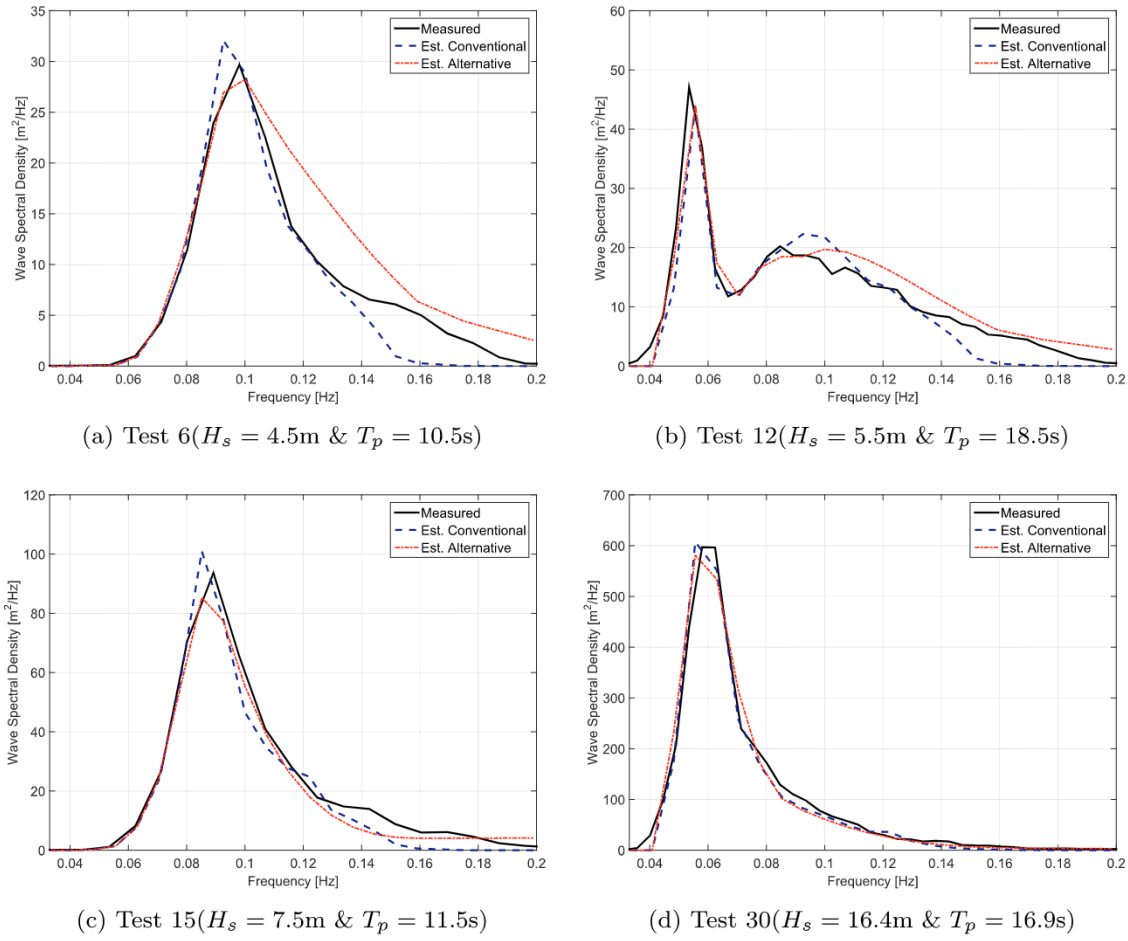

(a) Test 6($H_s = 4.5$m & $T_p = 10.5$s) (b) Test 12($H_s = 5.5$m & $T_p = 18.5$s)

(c) Test 15($H_s = 7.5$m & $T_p = 11.5$s) (d) Test 30($H_s = 16.4$m & $T_p = 16.9$s)

Fig. 11. 2D estimated sea spectra for heading 135°.

estimations obtained close to frequency ranges where more than one motion presents RAOs cancellation points. This improvement may be relevant for the use of other types of vessels for motion based measurement systems, such as FPSOs, whose motions are characterized for presenting several RAOs cancellation points in the wave frequency range of interest, that may lead to misleading estimations of the sea states if the conventional approach is adopted.

It is also important to highlight the proposed VMB requires a small optimal value for the third hyperparameter. This hyperparameter aims at avoiding the overestimation of the energy close to the limits of the frequency range of interest. Accounting for the RAOs nonlinearity related inaccuracies has been shown to be a suitable approach to avoid the estimation of too large amounts of energy in the frequency range where the platform motions are characterized by non-linear response amplitudes. The systematic assessment regarding the sensitivity of the prior distribution hyperparameters to the RAOs inaccuracies has been left as a future work, since it entails a dedicated experimental campaign including short-crested sea conditions. Another future work thread that arises from this study is the use of the RAOs inaccuracies in the approach proposed in [6], which incorporates the measurement from onboard wave-probes to improve the estimations in the high frequency range of the sea spectra, and will also include the use of the inaccuracies related to the RAOs of the wave-probes.

Overall, it is possible to conclude that the adoption of a methodology that takes into account the inaccuracies of the RAOs due to the linearization of the seakeeping problem may lead to improvement of the estimations obtained through the VMB. As a matter of fact, these improvements are linked to the sea conditions that excite the non-linear responses of the vessel motions adopted as motion-based wave sensors.

Declaration of Competing Interest

The authors declare that they have no known competing financial interests or personal relationships that could have appeared to influence the work reported in this paper.

Acknowledgments

Authors are indebted to Petrobras and Equinor for supporting USP's previous research on the VMB method and to the Brazilian National Petroleum Agency (ANP), responsible for the regulations under which such research was conducted. Alexandre Nicolaos Simos acknowledges the Brazilian National Council for Scientific and Technological Development (CNPq) for his research grant. Jordi Mas-Soler acknowledges his D.Sc. scholarship granted by the "*Coordenação de Aperfeiçoamento de Pessoal de Nível Superior*" - Brasil (CAPES) - Finance Code 001. Finally, Jordi Mas-Soler also would like to thank the financial support he has received from the ARCWIND project — Adaptation and implementation of floating wind energy conversion technology for the Atlantic region (EAPA 344/2016) — , which is co-financed by the European Regional Development Fund through the Interreg Atlantic Area Programme; and Prof. Antonio Souto-Iglesias for the fruitful discussions during the last stages of the writing of the paper.

Appendix A. Test Matrices: Regular Wave Specifications

Main features of the regular waves tested during the experimental campaign are included in the following table.

Table A1
Input parameters used for regular wave conditions.

Wave	$T_p(s)$	$H_s(m)$	Steepness (%)
W01	8,0	2,0	2
W02	9,6	2,9	2
W03	11,1	3,9	2
W04	12,7	5,0	2
W05	14,2	6,3	2
W06	15,8	7,8	2
W07	17,3	9,4	2
W08	18,9	11,1	2
W09	20,4	13,0	2
W10	22,0	15,1	2
W11	24,0	15,7	2
W12	8,0	4,0	4
W13	9,6	5,7	4
W14	11,1	7,7	4
W15	12,7	10,0	4
W16	14,2	12,6	4
W17	15,8	15,6	4
W18	17,3	18,8	4
W19	18,9	22,3	4
W20	20,4	26,1	4
W21	22,0	30,1	4
W22	8,0	6,0	6
W23	9,6	8,6	6
W24	11,1	11,6	6
W25	12,7	15,0	6
W26	14,2	18,9	6
W27	15,8	23,3	6
W28	17,3	28,0	6
W29	18,9	33,0	6
W30	20,4	37,1	6
W31	22,0	39,0	6

References

[1] H. Akaike, Likelihood and the bayes procedure, Trabajos de estadística y de investigación operativa 31 (1) (1980) 143–166.
[2] J. Bendat, Statistical errors in measurement of coherence functions and input/output quantities, J. Sound Vib. 59 (3) (1978) 405–421.
[3] I.B. Bispo, A.N. Queiroz Filho, E.A. Tannuri, A.N. Simos, Motion-based wave inference: Monitoring campaign on a turret fpso, The 35th International Conference on Ocean, Offshore and Arctic Engineering. OMAE2016, Busan, KR., 2016.
[4] A.H. Brodtkorb, U.D. Nielsen, A.J. Sørensen, Sea state estimation using vessel response in dynamic positioning, Appl. Ocean Res. 70 (2018) 76–86.
[5] M. Davis, E.E. Zarnick, Testing Ship Models in Transient Waves, Technical Report, David taylor model basin washington dc hydromechanics lab, 1966.
[6] F.L. de Souza, E.A. Tannuri, P.C. de Mello, G. Franzini, J. Mas-Soler, A.N. Simos, Bayesian estimation of directional wave-spectrum using vessel motions and wave-probes: proposal and preliminary experimental validation, J. Offshore Mech. Arct. Eng. 140 (4) (2018).
[7] K. Hasselmann, T. Barnett, E. Bouws, H. Carlson, D. Cartwright, K. Enke, J. Ewing, H. Gienapp, D. Hasselmann, P. Kruseman, et al., Measurements of wind-wave growth and swell decay during the joint north sea wave project (JONSWAP), Ergänzungsheft 8 (12) (1973) 95.
[8] T. Iseki, An improved stochastic modeling for bayesian wave estimation, The 31st International Conference on Ocean, Offshore and Arctic Engineering. OMAE2012, Rio de Janeiro, BR., 2012, pp. 455–461.
[9] T. Iseki, K. Ohtsu, Bayesian estimation of directional wave spectra based on ship motions, Control Eng Pract 8 (2) (2000) 215–219.
[10] C.-H. Lee, J.N. Newman, Wamit User Manual, WAMIT, Inc, 2006.
[11] B. Mak, B. Düz, Ship as a wave buoy - estimating relative wave direction from in-service ship motion measurements using machine learning, The 38th International Conference on Ocean, Offshore and Arctic Engineering. OMAE2019, Glasgow, Scotland, 2019.
[12] J. Mas-Soler, A.N. Simos, E.A. Tannuri, Estimating on-site wave spectra from the motions of a semi-submersible platform: an assessment based on model scale results, Ocean Eng. 153 (2018) 154–172.
[13] J. Newman, Marine Hydrodynamics, MIT Press, Cambridge, MA., 1977.
[14] U.D. Nielsen, A.H. Brodtkorb, A.J. Sørensen, Sea state estimation using multiple ships simultaneously as sailing wave buoys, Appl. Ocean Res. 83 (2019) 65–76.
[15] U.D. Nielsen, Introducing two hyperparameters in bayesian estimation of wave spectra, Probab. Eng. Mech. 23 (1) (2008) 84–94.
[16] B. Servan-Camas, J.E. Gutierrez-Romero, J. Garcia-Espinosa, A time-domain second-order FEM model for the wave diffraction-radiation problem. Validation with a semisubmersible platform, Mar. Struct. 58 (2018) 278–300.
[17] A.N. Simos, E.A. Tannuri, J.V. Sparano, V.L. Matos, Estimating wave spectra from the motions of moored vessels: experimental validation, Appl. Ocean Res. 32 (2) (2010) 191–208.
[18] A.N. Simos, E.A. Tannuri, J.J. da Cruz, A.N. Queiroz Filho, I.B. da Silva Bispo, R.C. Carvalho, Development of an on-board wave estimation system based on the motions of a moored FPSO: Commissioning and preliminary validation, The 31st International Conference on Ocean, Offshore and Arctic Engineering. OMAE2012, Rio de Janeiro, BR., 2012.
[19] C.G. Soares, Effect of transfer function uncertainty on short-term ship responses, Ocean Eng. 18 (4) (1991) 329–362.
[20] E.A. Tannuri, J.V. Sparano, A.N. Simos, J.J. Da Cruz, Estimating directional wave spectrum based on stationary ship motion measurements, Appl. Ocean Res. 25 (5) (2003) 243–261.
[21] K. Torsethaugen, S. Haver, Simplified double peak spectral model for ocean waves, The 14th International Offshore and Polar Engineering Conference. ISOPE2004, Toulon, FR., 2004.
[22] J. Mas-Soler, Assessing the Use of a Semisubmersible Oil Platform as a Motion-Based Sea Wave Sensor, Ph.D. Thesis, Escola Politécnica, University of São Paulo (USP) (2018), https://doi.org/10.11606/T.3.2019.tde-29052019-082426.
[23] J. Mas-Soler, A. Souto-Iglesias, A.N. Simos, et al., Assessing an Improved Bayesian Model for Directional Motion Based Wave Inference, J. Mar. Sci. Eng. 8 (4) (2020) 231.